

## FLOW ADAPTIVE AERODYNAMIC PROBE FOR TURBOMACHINERY FLOWS

C. Lenherr, M. Oswald, A.I. Kalfas, R.S. Abhari  
Turbomachinery Laboratory  
Swiss Federal Institute of Technology, ETH Zurich  
Switzerland

### ABSTRACT

In order to enable turbomachinery research to obtain data highly resolved in space and time, a novel flow adaptive aerodynamic probe concept has been developed and presented in this paper. The algorithm selects the measurement positions of the probe automatically and therefore provides higher measurement fidelity compared to traditional methods.

The development of the adaptive algorithm has been done in several steps. First an automatic 1D-traversing algorithm has been developed. The following steps dealt with the subject of a 2D adaptive flow concept development, whereas primarily visual programming language-computer package simulations of the new 2D algorithm have been done based on data from previous test series at the Turbomachinery Laboratory.

The new 2D traversing algorithm is fully self-controlled and requires minimal input such as blade count and hub and tip diameters. Furthermore, areas of interest (e.g. secondary flows, wake) are detected automatically and higher measuring point resolutions are ensured in these regions.

After the successful simulations, the intelligent 2D algorithm has been adapted to an object oriented programming environment used for automated data acquisition and reduction. An evaluation of the flow adaptive aerodynamic flow concept has been done on a pressure turbine facility by means of a steady pneumatic probe. The measurement results show that the new 2D algorithm has the potential to detect new flow phenomena. In contrast to traditional algorithms, which in case of a possible enhancement demand a knowledge of the position of interesting areas such as the wake and vortical structures before starting the measurement, the new algorithm detects the right areas and enhances the resolution fully self controlled in these areas.

Furthermore, the new 2D flow adaptive probe concept shows a significant improvement regarding the needed time for one measurement.

### NOMENCLATURE

$C_{pt}$	Total Pressure Coefficient	[-]
	$\frac{P_{tot} - P_{stat,Exit}}{P_{tot,Inlet} - P_{stat,Exit}}$	
M	Mach Number	[-]
$P_{atm}$	Atmospheric Pressure	[Pa]
$P_{stat}$	Static Pressure	[Pa]
$P_{tot}$	Total Pressure	[Pa]
$\alpha$	Flow Yaw Angle	[°]
$\beta$	Flow Pitch Angle	[°]
d	Distance	[m]

### Subscripts

i	Index, Counter
x	Axial direction
$\theta$	Circumferential
r	Radial

### Abbreviations

D	Dimensional
DF	Detection Function
FP	Flow property value
PS	Blade Pressure Side
SS	Blade Suction Side

### INTRODUCTION

The analysis, prediction, understanding and control of turbomachinery flows, such as wakes and vortices, are major issues in modern turbomachinery design.

For further turbomachinery development a deep understanding of the complex flow mechanisms is needed. To achieve that, Computational Fluid Dynamic (CFD) is used as well as experimental methods. Especially traditional experiments, using time-averaged methods, are replaced more and more by numerical calculations for financial reasons. Present CFD-

codes are limited by their computing power. Calculating unsteady flow features needs even more computing power than calculating on a time independent way. Due to the general interest to develop CFD tools, which predict the unsteady flow behavior in an even more accurate way, progressive measurement methods still remain very important. Therefore, the last two decades of development have shown a strong interest in probe measuring techniques.

Point measuring methods often need a great deal of additional effort including extra measuring loops to get the approximate flow angles, writing of positioning task files, or a manual start of the traverses. An algorithm that finds it's own way through an unsteady flow field fully self-controlled in 2 directions can reduce these additional efforts.

It is, generally, possible to work with a predefined uniform measuring grid. In case of a possible local refinement, advanced prior knowledge of the position of the wake and vortex structures is necessary.

The required inputs for running a test should be minimal. By decreasing the dependency of a measurement algorithm from the test facility, the measuring system can easily be adapted to any facility.

Additional goals are a reduction of the required time for one test and at the same time a higher measuring point resolution at areas of interest, where secondary flow effects as wake and vortex structures occur.

Lienert [1] and Marti [2] started with the first development step of a progressive traversing algorithm, that defines a traversing and measurement strategy for 3D flow structures. The algorithm allowed more efficient data acquisition by focusing especially on areas that require higher spatial resolution. This algorithm traversed the probe automatically step by step from tip to hub and measured the flow properties at each radial position using the previous yaw angle  $\alpha$  as an input for the following traverse point. After finishing one traverse, critical areas were detected by means of a suitable detection function and an array of locally improved radial positions was generated. A re-measurement, done at the new gained positions gave new flow-information, which were inserted into the previous ones. Oswald [3] improved the algorithm and made it fully self controlled in radial direction. The first part of the 1D progressive algorithm is a uniform traversing. Then a detection function is used to decide the location of additional points in radial direction. Fig 1 shows the yaw angle distribution over one pitch resulting of unsteady probe measurements.

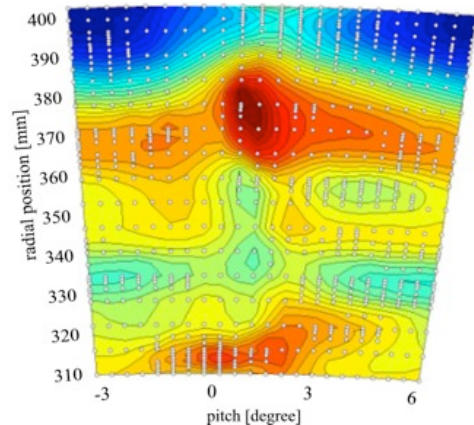


Fig 1: Yaw angle distribuion out of 1D progressive traversing algorithm

A comparison to the current state of the art method (2D measurements by means of a uniform grid where no refinement is possible) used at the LSM showed that the 1D algorithm is about 30% faster.

Some important properties of the 1D Progressive Traversing Algorithm, applied on the experimental research facility "LISA", can be seen in Fig 2 and Table 1.

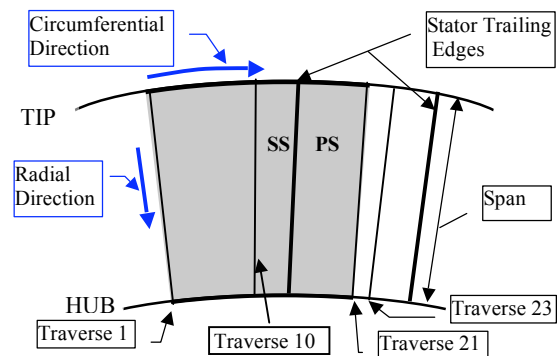


Fig 2: Measurement Area (one pitch)

Properties of the 1D (radial) Progressive Traversing Algorithm
<ul style="list-style-type: none"> <li>•Uniform starting grid Initialization: <ul style="list-style-type: none"> <li>- 16 radial points per Traverse</li> <li>- 23 circumferential positions (Traverses)</li> </ul> </li> </ul>
<ul style="list-style-type: none"> <li>•3 enhancement loops (in radial direction)</li> </ul>
<ul style="list-style-type: none"> <li>•Number of measured points after 3rd loop: 776</li> </ul>
<ul style="list-style-type: none"> <li>•Total time for a complete test loop: ~12 hrs.</li> </ul>

Table 1: 1D Progressive Traversing Algorithm

At a further step in the development of adaptive flow algorithms, a 2D traversing algorithm was developed [4].

This new method can and has been used with both pneumatic and fast response probes. As an example, in clocking the structures defining the areas of interest move. The movement is not always proportional to the clocking angle [5]. In this case,

the self-guided intelligent probe algorithm adjusts the measured points to the flow field. The resultant measured flow fields are compared in a de facto unbiased fashion.

The 2D traversing algorithm is fully automatic in both radial and circumferential direction. This is addressed in the first part of the paper. A further section describes the instrumentation and research facility that was used to evaluate the newly developed 2D algorithm. In the final section of the paper, the results of the tests are presented and discussed.

## 2D ADAPTIVE TRAVERSING ALGORITHM

The 2D adaptive algorithm is structured in a pre-processing section, a main-processing section and a post-processing section (Fig 3).

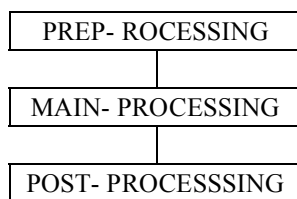


Fig 3: 2D traversing algorithm structure

Oschwald's [3] 1D traversing algorithm detected points of interest for radial traverses with the strategy to add some measurement points on a lower radial position of a detected point of interest. The 2D algorithm adds next to a lower radial position of a detected point also points on a higher on. Furthermore, it works in an additional dimension (circumferential) and enhances at the left hand side and the right hand side respectively of a point of interest (Fig 4).

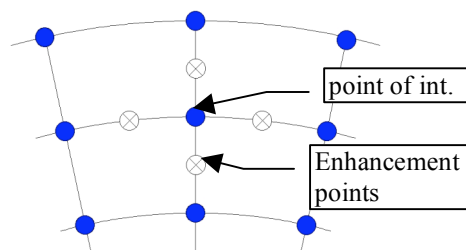


Fig 4: 2D Concept measuring structure

Parts of the algorithm development have happened using unsteady probes. Therefore the same algorithm can be used to find points of interest by means of a number of criteria including unsteady and loss significant quantities such as turbulence intensity  $Tu$ , deterministic and random pressures respectively [6], [7], [8].

### PRE- PROCESSING

The main goal of a progressive algorithm is to find points of interest in a measurement area and increase then the number of measured points at

areas of interest fully self controlled. However, in order to be able to make a weighting about areas of interest, first a certain amount of points in the flow field has to be measured. This is done in the algorithm main section by means of a uniform start grid that covers the whole measurement pitch. Using adaptive algorithms that start from a uniform grid is well known out of CFD adaptive meshing methods and is therefore legitimated for progressive probe measuring techniques [9].

The dimensions of the uniform start grid mainly depend on geometrical parameters of the facility. On one hand, it should not be too small, to avoid an important loss of flow feature information and on the other hand, it should not be too dense, that a sufficient lead is given for increasing at the detected points of interest without running the risk that a complete algorithm run-through takes infeasible much time. Experimental investigation [4] of the minimal number of measurement points needed in a pitch to asses the overall loss of important flow feature information on the 2-stage axial research turbine "LISA" was performed. It has been shown that the dimension of the uniform starting grid for the 2D adaptive flow concept of the order  $10^2$  lead to accurate assessment of the total pressure distribution.

The pre-processing section of the algorithm is used to define the specific size of the starting grid and the size of the finest possible measurement grid. The size of the finest grid is dependent on measurement time constrains and the probe head size and geometry. In the algorithm the finest grid is used for interpolation constrains that have to be done during the run in each loop and is addressed in the main-processing and post-processing section respectively of the paper.

### MAIN- PROCESSING

The execution of the points during one algorithm run is controlled in the main-processing section. Three stepper motors handle the particular positioning of the probe in the measurement area, controlling the radial, circumferential and probe roll, respectively.

As initial step of the main-processing section, the uniform start grid is measured as defined in the pre-processing.

The enhancement sections of the algorithm can be called up based on the structured start grid. Three enhancement loops have been defined, which differ from each other on the detection functions (DF). These detection functions accord to the various criteria that particular find the points of interest regarding all measured points [10]. The user can adapt these criteria depending on the investigations main focus.

To assure a certain flexibility regarding the investigation for the user, the number of enhancement loops for each section and the number

of points that should be measured per loop can be defined. In addition, to the limitation of the measuring point number, some other termination criteria are defined based on maximal and minimal distances between points of interest and their neighboring points. These distance criteria are the same for all three sections. They control the distance between two measured neighboring points and allow inserting a new measurement point if the above distances are not smaller than a certain value related to traversing system uncertainties and the used probe head diameter. If the distance between two neighboring points is larger than a certain value, the algorithm does not position the point being measured on the central point of the two neighboring points, but with a certain distance to the detected point of interest. This ensures that new measured points around a point of interest are positioned in the particular area of interest.

The insertion of measurement points leads to an unstructured grid, however, due to numerical constraints the detection functions need to be applied on a structured grid. Therefore, after each loop of the algorithm, the unstructured grid is interpolated on a structured utility grid that has the dimensions of the finest possible grid. This interpolation is done by means of a distance weighted mean averaging.

The detection functions then are applied on the interpolated utility grid. The results of the particular detection functions applied on the grid are filtered based on the measured points and allow the detection of new points of interest.

In the paper, the three different sections of the main process are called “pressure\_min”, “pressure\_gradient” and “yawangle\_criterion”.

A wake behind a blade is created due to boundary layer effects. One characteristic of a wake is therefore smaller velocity components then in regions outside of the wake area. Due to that loss in velocity in the wake area, the total pressure of the area is smaller then in regions around the wake. Therefore the two sections “pressure\_min” and “pressure\_gradient” are used to ensure a high accuracy regarding the representation of flow characteristics such as the wake.

Binder et al. [11] showed that the yaw angle seems to be a suitable indicator for the detection of wakes and specially vortices in a passage behind a stator, whereas the pitch angle  $\beta$  would not be a good detection instrument for vortices and wakes. This has to do with the characteristic velocity profile of a stator blade wake that is more or less two-dimensional and therefore varies little in span direction. Therefore the “yawangle\_criterion” is used to detect further flow features, such as vortical structures, that cannot necessarily be detected by total pressure criteria.

A certain number of local minima of measured total pressures are found by the detection function

of “pressure\_min”. Guidelines to limit or terminate the “pressure\_min” detection function are given by the distance criterion and the total number of measurement points limitation respectively.

The section “pressure\_gradient” enhances by means of two criteria considering the total pressure gradients in the radial (eq. 1) and the circumferential direction (eq. 3) of all points that have been measured up to that step. The points of interest are found by means of thresholds, regarding the average of the gradients in the two directions over all measured and interpolated points  $m$  (eq. 2 and eq. 4). The values of the different thresholds are compared to the values of the corresponding detection functions at the different measured positions. If the value of the detection function at a certain position is larger than the value of the threshold, this position is defined as an area of interest.

$$DF(r) = \left( \frac{\partial P_{tot}}{\partial r} \right)^2 \quad (1)$$

$$Threshold\ 1 = \frac{1}{m} \cdot \sum_{i=1}^m \left( DF(r)_{point\ i} \right) \quad (2)$$

$$DF(\theta) = \left( \frac{\partial P_{tot}}{\partial \theta} \right)^2 \quad (3)$$

$$Threshold\ 2 = \frac{1}{m} \cdot \sum_{i=1}^m \left( DF(\theta)_{point\ i} \right) \quad (4)$$

The gradients are squared to smooth out fluctuations for the different positions, which qualitatively improves the detection of the points with high gradients.

The growth of points that are investigated further is fixed to assure space for later algorithm sections regarding other criteria. Additionally, the distance criterion is used in the section “pressure\_gradient”.

Two detection functions are used in the section “yawangle\_criterion” of the 2D progressive algorithm (eq. 5 and eq. 7). The points of interest are found by means of thresholds over all measured and interpolated points  $m$ , regarding the average of the different detection functions over the structured matrices (eq. 6 and eq. 8). The value of each threshold is compared to the values of the corresponding detection function at the different measured positions. If the value of the detection function at a certain position is larger than the value of the threshold, this position is defined as an area of interest.

The detection functions and the thresholds are defined as follows:

$$DF1 = \left( \frac{\partial \alpha}{\partial r} \right)^2 \cdot \left( \frac{\partial \alpha}{\partial \theta} \right)^2 \quad (5)$$

$$Threshold\ 1 = \frac{1}{m} \cdot \sum_{i=1}^m (DF1_i) \quad (6)$$

$$DF2 = \left( \frac{\partial^2 \alpha}{\partial r^2} \right)^2 \cdot \left( \frac{\partial^2 \alpha}{\partial \theta^2} \right)^2 \quad (7)$$

$$Threshold\ 2 = \frac{1}{m} \cdot \sum_{i=1}^m (DF2_i) \quad (8)$$

Again, the detection functions are squares of first or second derivatives respectively, to smooth out fluctuations for the different positions, what qualitatively improves the detection of the points of interest. In section “yawangle\_criterion”, the same kind of termination criteria is used as in the previous sections.

The general structure for all three sections is similar. An overview about the structure of such a section is given in Fig 5.

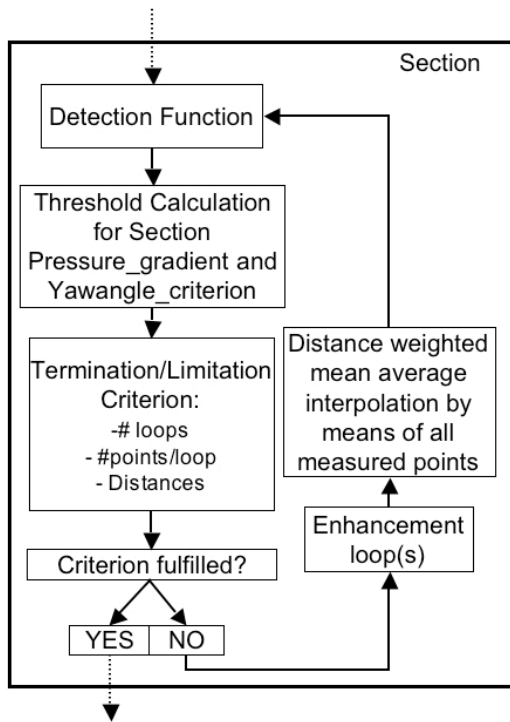


Fig 5: Section structure

## POST- PROCESSING

The developed algorithm starts with “few” measurement points and then the number of measured points increases by measuring at areas of interest. This could bring out some issues when compared to measurements done by means of a sufficiently dense uniform grid. These issues are mainly related to the post- processing of the parameters measured or simulated respectively at the points of interest. If one just measures at points

in a pitch that build up a uniform grid, the measurement parameters build fully filled matrices that can be easily post processed. This is not the case for a progressive 2D algorithm because one enhances at local areas around points of interest. The data have to be interpolated to allow a post processing. That interpolation consists out of two steps. Initially, 1D cubic spline interpolations are done on the boundary of the defined measurement area. As a second step, each position is detected, that has to be interpolated. After that, the detected positions are worked through in a loop, whereas a local coordinate system is positioned in the particular points  $(x_0, y_0)$ . Afterwards in each of the quadrants (Quadr) of the local coordinate system, the closest measurement point to the local zero is identified. The flow property value (FP) for a particular detected point is calculated by means of a distance weighted mean average of the flow properties of the four closest measurement points  $(FP_{1,Quad}$  to  $FP_{4,Quad}$ ) (eq. 9).

$$FP_{(x_0=y_0=0)} = \frac{\frac{FP_{1,Quad}}{d_1} + \frac{FP_{2,Quad}}{d_2} + \frac{FP_{3,Quad}}{d_3} + \frac{FP_{4,Quad}}{d_4}}{\sum_{i=1}^4 \frac{1}{d_i}} \quad (9)$$

Furthermore, the post- processing shows an additional feature that allows defining further points that the user wishes to be measured.

## EXPERIMENTAL EVALUATION OF THE TECHNIQUE

### INSTRUMENTATION

The flow adaptive aerodynamic flow concept is evaluated by means of a pneumatic cobra-shaped 5-Hole probe [12] and Fast Response Aerodynamic Probes (FRAP) [13].

The cobra-shaped 5-Hole probe has a calibration range of  $\pm 12^\circ$  in yaw and  $\pm 30^\circ$  in pitch angle. The probe head has a diameter of 0.9mm and the tip is slanted pyramid shaped (Fig 6).

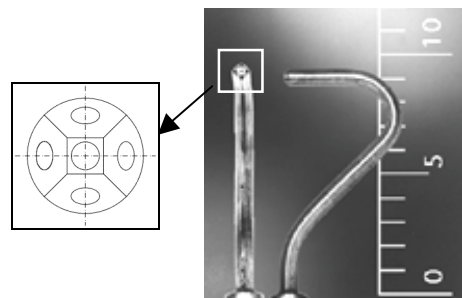


Fig 6: Cobra-Shaped 5-Hole Probe

By means of a 5-hole probe, following flow properties can be measured on a steady way:

—>  $\alpha$ ,  $\beta$ ,  $P_{tot}$ ,  $P_{stat}$ ,  $M$

The used Fast Response Aerodynamic Probe is a single, temperature compensated sensor probe. The aspect ratio of the elliptical probe head is 2:1, the pressure tab angle is 0 and about 1.8 mm apart from the probe tip. The probe head has a diameter of 1.8mm. Tanaka et al. [14] presented a systematic evaluation of the pitch sensitivity for different probe heads. Some more general information about Fast Response Aerodynamic Probes can be found in Gossweiler et al. [15], Humm et al. [16], and Kupferschmied et al. [17].



Fig 7: Fast Response Aerodynamic Probe

The sign convention for a positive yaw angle defines that it directs to the rotor sense of rotation (y-axis), and for a positive pitch angle to the blade tip (z-axis). The main flow in Fig 8 is directed in the negative x-axis direction.

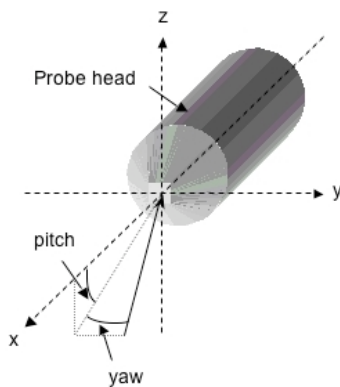


Fig 8: Yaw and Pitch Angle convention

## RESEARCH FACILITY

The 2D adaptive flow concept has been applied to the experimental research facility "LISA" [18]. Some of the characteristic parameters of the turbine for this application are given in Table 2.

Parameter	Value
Rotational Speed	2500 RPM
Pressure Ratio	1.34
Aspect Ratio (Span/Ax. Chord)	1.8
Blade Count (Rotor/Stator)	42 / 42
Outer Tip Diameter	0.8m
Massflow	10.26 kg/s
Typical Turbine Entry Temperature	45°C

Table 2: Characteristic turbine parameters

The area behind the second stator of the 2-stage axial research turbine has been chosen as measurement position for the evaluation of the 2D adaptive flow concept (Fig 9).

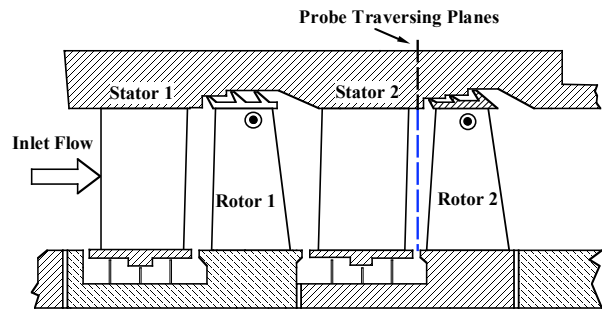


Fig 9: Measurement position after 2<sup>nd</sup> stator

## RESULTS

The 2D adaptive aerodynamic probe concept is evaluated by means of two pneumatic probe measurements on a 2-stage axial research turbine. Next to the 2D adaptive concept measurements, one measurement has been done by means of a uniform grid (23 x 30) with 23 traverses in circumferential direction and 30 measurement points per half span.

The two 2D adaptive probe concept measurements differ from each other in the number of loops and the number of points per loop respectively. Table 3 and Table 4 show the loop number and the number of points that are measured per loop for these two different test series:

Measurement 1:			
Section:	No of loops	No of points/loop	Total No of points
<b>MAIN PROCESS:</b>			
Uniform Start Grid 8x11	1	88	88
Pressure_min	3	50	150
Pressure_gradient	2	40	80
Yawangle_criterion	4	50	200
<b>POST PROCESS:</b>			
No additional measurement points are defined.			

Table 3: Parameters for the 2D adaptive probe concept measurement 1

The uniform grid that is measured to compare with the data of the 2D adaptive algorithm consists out of 690 measurement points. The selected configuration for measurement one with the 2D adaptive flow concept has a total measurement point size of 518 points. Due to the distance criteria, in the section pressure\_min the algorithm measured 118 points, in pressure\_gradient 64 points, and in the yawangle\_criterion 84 points. Therefore, the adaptive algorithm didn't measure 518 but 354 points in measurement 1.

<b>Measurement 2:</b>			
<b>Section:</b>	<b>No of loops</b>	<b>No of points/loop</b>	<b>Total No of points</b>
<b>MAIN PROCESS:</b>			
Uniform Start Grid 8x11	1	88	88
Pressure_min	4	50	200
Pressure_gradient	4	40	160
Yawangle_criterion	4	40	160
<b>POST PROCESS:</b>			
No additional measurement points are defined.			

Table 4: Parameters for the 2D adaptive probe concept measurement 2

The selected configuration for measurement two with the 2D adaptive flow concept has a total measurement point size of 608 points.

Due to the distance criteria, in section pressure\_min 145 points have been measured, in section pressure\_gradient 131 points, and in the section yawangle\_criterion 147 points. Therefore, the adaptive algorithm didn't measure 608 but 513 points in measurement 2. Regarding the total number of measurement points for measurement 2, the gain in time compared to the uniform grid measurement is small. Anyway, measurement 2 has been done to see how that the algorithm enhancement works in an environment that already has a certain density.

Yaw angle  $\alpha$  and the total pressure  $P_{tot}$  are the flow properties that are used in the different detection functions. Therefore the presented measurement results focus on these two properties or properties that are affiliated out of them.

**Total Pressure Coefficient  $C_{pt}$ , measurement 1**

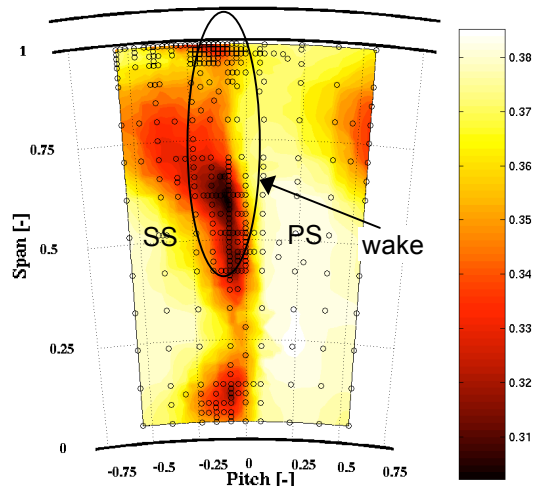


Fig 10:  $C_{pt}$  [-] distribution resulting from flow adaptive probe concept, measurement 1

**Yaw Angle  $\alpha$ , measurement 1**

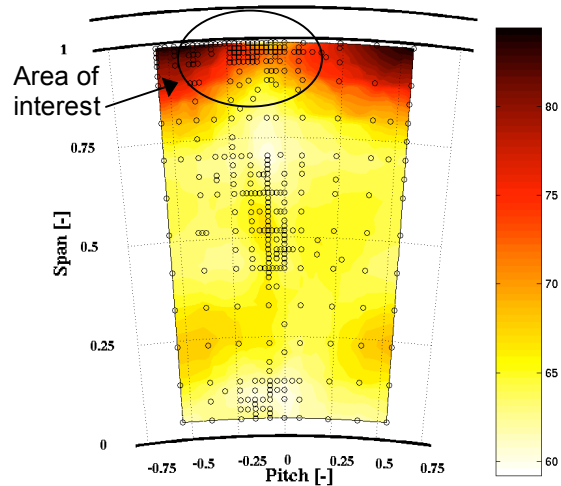


Fig 12:  $\alpha$  [°] distribution resulting from flow adaptive probe concept, measurement 1

**Total Pressure Coefficient  $C_{pt}$ , measurement 2**

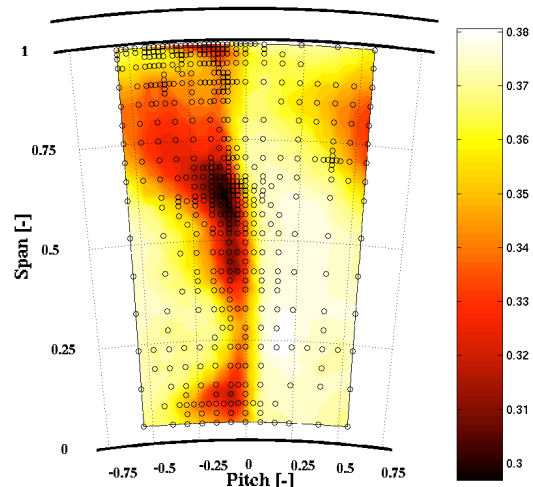


Fig 11:  $C_{pt}$  [-] distribution resulting from flow adaptive probe concept, measurement 2

**Yaw Angle  $\alpha$ , measurement 2**

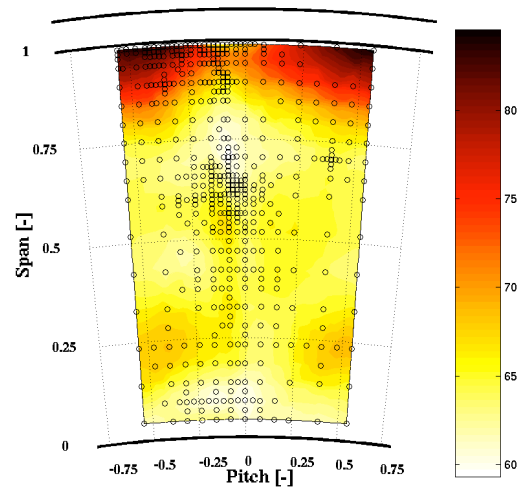


Fig 13:  $\alpha$  [°] distribution resulting from flow adaptive probe concept, measurement 2

Fig 10 and Fig 11 show the total pressure coefficient distribution over a pitch at the end of the algorithm run for measurement 1 and measurement 2 respectively.

In Fig 12 and Fig 13, the yaw angle distribution over one pitch at the end of the algorithm run for measurement 1 and measurement 2 respectively are presented.

In all the figures, the geometrical locations where measurements have been done during the algorithm are visualized by small circular marks.

Intrusive measurement techniques in rotating environments lead to additional safety factors that have to be considered. Touching rotating parts of the turbine with the probe during measurements would immediately damage the probe or even lead to an emergency shut down of the facility. To avoid such an accident, additional safety distances are defined between the measurement position with the lowest radius and the rotor hub. Therefore, all figures show a not measured and white zone around 0% to 5% span. Another unmeasured zone is located in the tip region, between 99% span and 100% span. The reason for this unmeasured zone in the tip region has nothing to do with safety distances but with probe calibration range limitations. In this region, the fluctuations in yaw angle are very strong due to tip leakage flows. The fluctuation range in these regions exceeds the calibration range of the used cobra shaped 5-hole probe and illegitimated flow angles would result.

The difference in the number of measured points between measurement 1 and measurement 2 can clearly be seen by comparing Fig 10 with Fig 11 as well as Fig 12 with Fig 13. Although the difference in measured points between measurement 1 and measurement 2 is 159 points, there is no significant difference regarding the flow property distribution result over the whole pitch for the two measurements.

Regarding the location of the measured points, Fig 10 shows that the algorithm enhances at areas with low total pressure coefficients, what generally indicates the location of a wake. The same can be seen in Fig 11. The only difference to Fig 10 is the higher measurement point density in the wake and in the local area around the wake, what has to do with the fact that the algorithm was allowed to find more points for the sections `pressure_min` and `pressure_gradient` in measurement 2. Exactly the same characteristic can be seen comparing Fig 12 with Fig 13. Regarding the yaw angle distribution, the main area of interest is situated in the upper 25% span of the pitch (see Fig 12). Vortical structures are expected in this area due to tip leakage flow. These areas of interest are for both measurements detected during the run of the section `yawangle_criterion`.

Fig 14 to Fig 19 show a closer view to the upper 50% span of a pitch to allow a more detailed

discussion about the qualitative flow results out of the two adaptive flow measurement series.

For comparatively reasons, next to the results for the total pressure coefficient distribution and the yaw angle distribution for measurement 1 and measurement 2 respectively, the upper 50% span for the same flow properties are presented that resulted out of a uniform grid measurement. Fig 14 (I a) shows the total pressure coefficient distribution in the upper 50% span and Fig 17 (II a) the yaw angle distribution in the upper 50% span resulting out of the uniform grid measurement. This uniform grid was measured with 23 circumferential traverses, whereas each traverse contained 30 measurement points in radial direction between blade mid span and the tip.

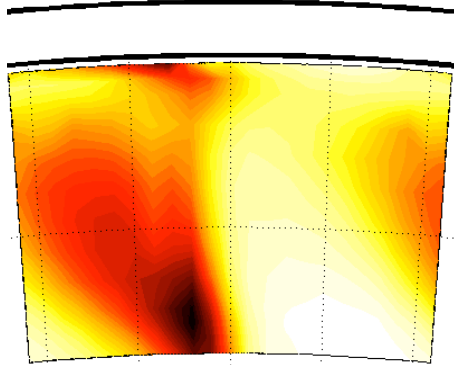
Fig 15 (I b) presents the total pressure coefficient distribution and Fig 18 (II b) the yaw angle distribution in the upper 50% span resulting out of the 2D adaptive probe concept measurement 1. The same two flow properties are presented in the similar area range in Fig 16 (I c) and Fig 19 (II c) but for the results out of the 2D adaptive probe concept measurement 2.

The flow results for the two total pressure coefficient plots, named with roman number I b and I c, show a good agreement to the uniform grid result I a. The two main areas of interest with a more dense measurement point resolution are at around 60% span and 90% span. It can be assumed that the area of interest around 60% span is highly influenced by the wake and the area around 90% span is influenced by vortical structures.

After measuring a certain amount of points in areas of interest and several enhancement steps, the measurement point density in this area reach the maxima, given by the distance criterion. Therefore later algorithm loops are not allowed to measure in the regions again, what automatically leads to a measurement point distribution over the whole pitch, what can be seen by comparing II b and II c.

The measurements with the 2D adaptive probe concept lead to an unstructured measurement point distribution over a pitch. To enable post processing by means of a visual programming language, the unstructured grid is interpolated. This interpolation is done by means of a distance weighted mean averaging for both adaptive probe concept measurements. The flow properties resulting out of the structured uniform grid 23 x 30 measurement have not to be interpolated. Therefore a slight shape difference can be seen between the plots for the uniform grid and the plots for the adaptive flow concept measurements. This difference could eventually be minimized in a further step, by using an interpolation- or averaging-method of a higher order.

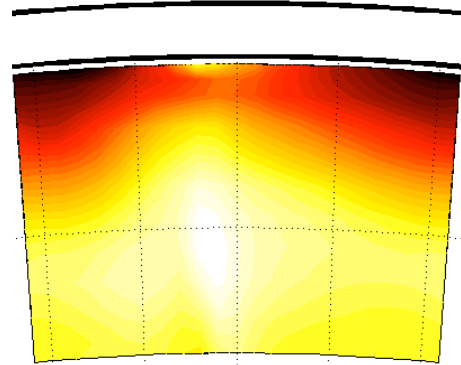
**Uniform Grid 23 x 30**  
**Total Pressure Coefficient  $C_{pt}$**



**I a**

*Fig 14: Upper 50% span of  $C_{pt}$  [-] distribution over one pitch measured by means of a uniform grid 23x30*

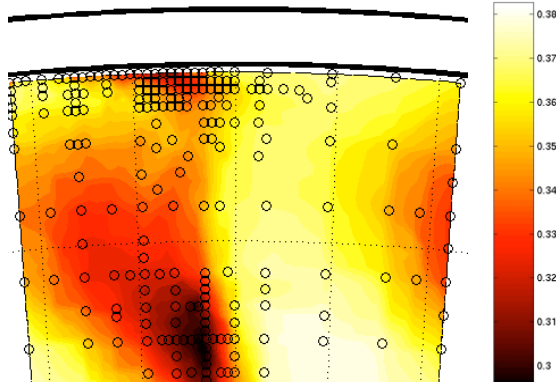
**Uniform Grid 23 x 30**  
**Yaw Angle  $\alpha$**



**II a**

*Fig 17: Upper 50% span of  $\alpha$  [°] distribution over one pitch measured by means of a uniform grid 23x30*

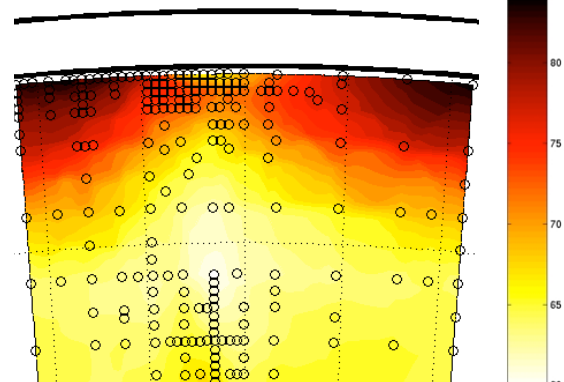
**Flow Adaptive Probe Concept**  
**Total Pressure Coefficient  $C_{pt}$ , measurements 1**



**I b**

*Fig 15: Upper 50% span of  $C_{pt}$  [-] distribution over one pitch measured by means of flow adaptive aerodynamic probe concept, measurement 1*

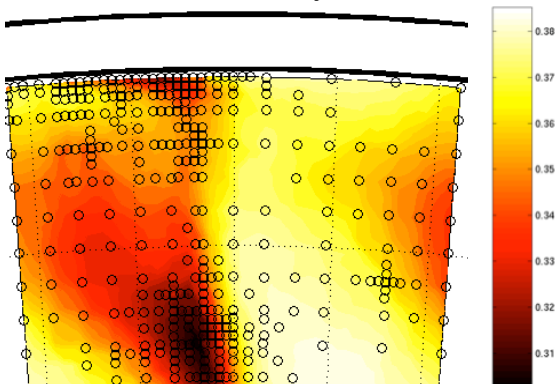
**Flow Adaptive Probe Concept**  
**Yaw Angle  $\alpha$ , measurements 1**



**II b**

*Fig 18: Upper 50% span of  $\alpha$  [°] distribution over one pitch measured by means of flow adaptive aerodynamic probe concept, measurement 1*

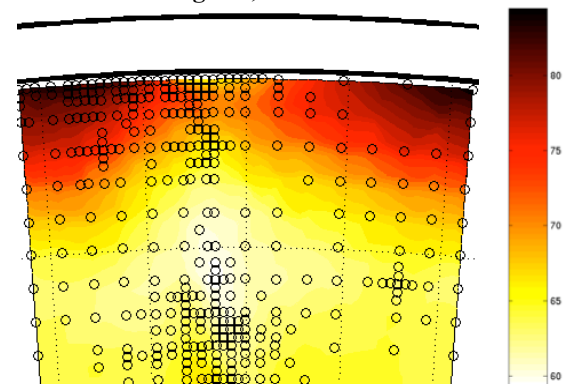
**Flow Adaptive Probe Concept**  
**Total Pressure Coefficient  $C_{pt}$ , measurements 2**



**I c**

*Fig 16: Upper 50% span of  $C_{pt}$  [-] distribution over one pitch measured by means of flow adaptive aerodynamic probe concept, measurement 2*

**Flow Adaptive Probe Concept**  
**Yaw Angle  $\alpha$ , measurements 2**



**II c**

*Fig 19: Upper 50% span of  $\alpha$  [°] distribution over one pitch measured by means of flow adaptive aerodynamic probe concept, measurement 2*

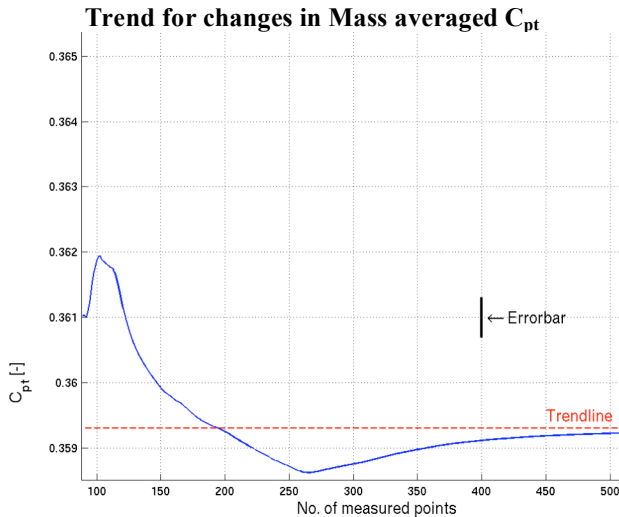


Fig 20: Mass averaged total pressure coefficient  $C_{pt}$  [-] for different number of measurement points

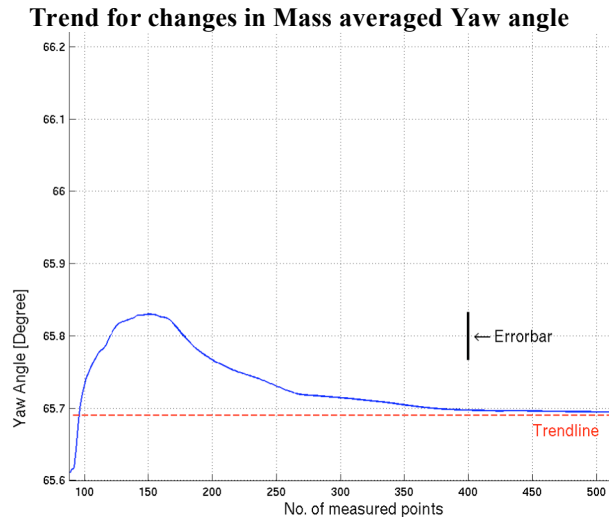


Fig 21: Mass averaged Yaw angle  $\alpha$  [°] for different number of measurement points

The measurement time for the 23x30 uniform grid was about 4 hours. The 2D adaptive flow concept measurement 1 lasted about 1 hour and 30 minutes and measurement 2 about 3 hours. As expected, regarding the total number of points, measurement 2 does not show a big gain in measurement time compared to the uniform grid.

The gain in measurement time for measurement 1 compared to the uniform state of the art method is in the range of about 63%.

Fig 20 and Fig 21 show the trend for changes in mass averaged total pressure coefficient and mass averaged yaw angle respectively for different numbers of measured points. This figures show, that the change for both, yaw angle and  $C_{pt}$  after around 300 measurement points is smaller than the range of the error bar for 5-H probe measurements.

Therefore, the use of the 2D adaptive probe concept with around 300 measurement points to get the same qualitative flow field information as for a uniform grid measurement with 690 points is legitimated.

The flow property development for one run-through of the algorithm is given in Fig 22 for measurement 1.

The flow variables total pressure coefficient and yaw angle respectively are presented over a full pitch. The respective variables are presented at the end of each of the four algorithm sections, “uniform grid”, “pressure\_min”, “pressure\_gradient” and “yawangle\_criterion”. Each of the plots show the respective flow variable and, with black circular marks, the total number of measured positions up to the actual loop in the algorithm.

From the start of the algorithm to the end of section “pressure\_gradient” the improvement over the full pitch is related to local total pressure minima and total pressure gradients respectively. If one compares the total pressure distribution at the end of section “pressure\_gradient” (I c) with the total pressure distribution of the uniform grid measurement by means of a structured 23 x 30 grid, it can be seen a good accordance of the total pressure distribution.

A characteristic for the location of a wake is a local low total pressure and local low total pressure coefficients respectively. As can be seen in the figures, the algorithm detects this area. Therefore, the points that have been inserted help for a better resolution of the overall pitch wise flow field.

The investigated points in section “yawangle\_criterion” are related to detection functions that consider the yaw angle distribution over the full pitch. In this last section, the points are mainly added in the area around the tip and some in the region around the hub. This has mainly to do with passage vortices in the hub and the tip region. Another flow effect that can influence the vortical structures in the tip regions is the tip leakage flow. All these flow phenomena can induce fluctuations in flow angles. The areas where such effects occur are localized by the detection functions of the section “yawangle\_criterion”.

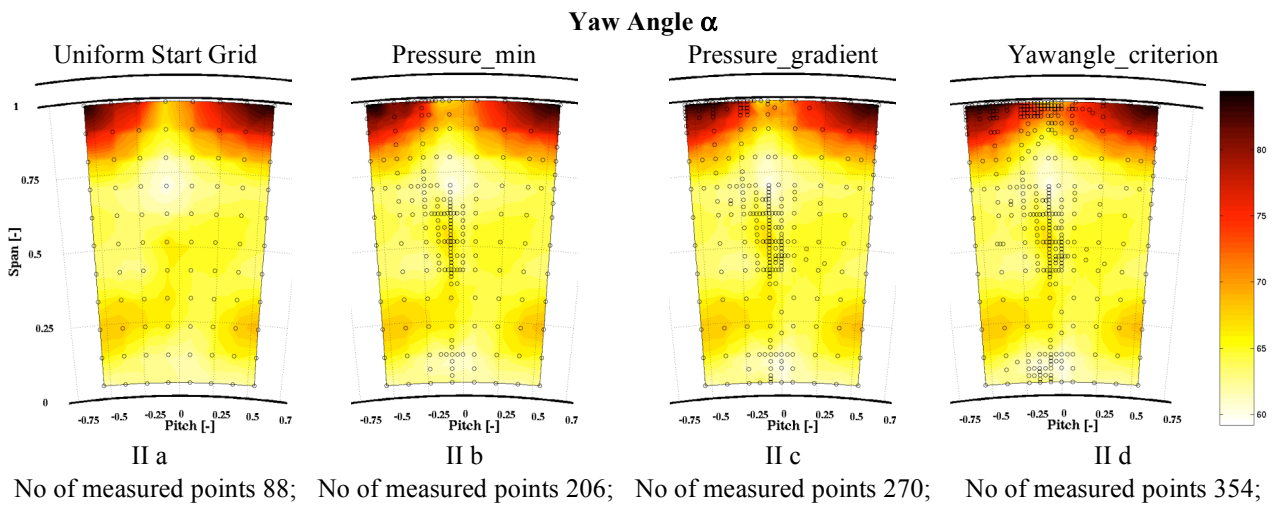
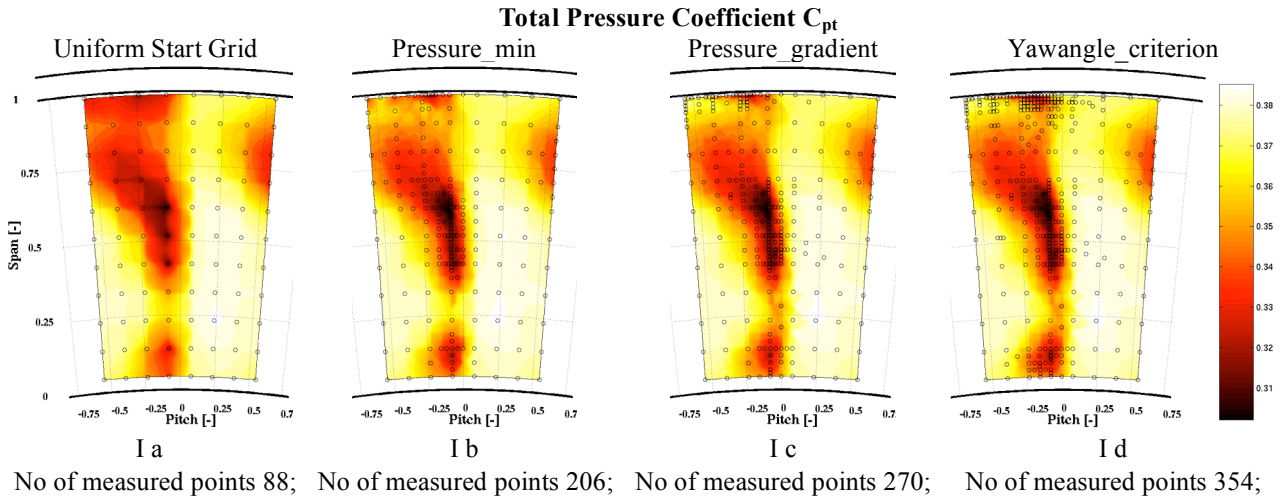


*Fig 22: Development of  $C_{pt}$  [-] and  $\alpha$  [°] distribution over one pitch during a run of the 2D adaptive aerodynamic probe concept (measurement 1)*

## CONCLUSIONS

A novel flow adaptive 2D flow concept has been developed. The new algorithm detects the right areas and enhances fully self-controlled at these areas of interest. The novel concept can be used for pneumatic probe measurements as well as for unsteady Fast Response Aerodynamic Probe measurements.

The 2D flow adaptive probe concept needs a minimal number of inputs such as blade count and hub and tip diameters. It can therefore easily be adapted to unknown facility or can be used in the development of new blade designs. In this case, flow features that were unknown before, can be found experimentally without any prior knowledge about their location, size or even their existence. The algorithm allows finding of areas of interest in such unknown conditions without extra measuring loops to get a certain knowledge about approximate flow angles. The additional efforts for intrusive probe measurements are therefore, significantly reduced.

The combinations of the different detection functions and stop criteria that are used to find areas of interest during the execution represent a good method for measuring by means of a 2D progressive traversing algorithm. The algorithm finds at least as many flow phenomena as alternative measurement techniques using structured grids.

The evaluation results have shown that a number of measurement points have been added successfully around the areas of interest.

One of the issues to investigate further deals with the different interpolation steps during an execution. The needed 2D interpolation in the post-processing of an adaptive 2D flow concept has a significant influence on the quality of the results.

The flow adaptive aerodynamic probe concept requires much less measuring points than state of the art methods. Using half the amount of measurement points compared to state of the art methods, results to qualitative comparable flow fields. This has a significant influence on the measuring time and the flow adaptive algorithm

therefore is about 63% faster than comparable techniques that use a uniform measurement grid (23 x 30). This measurement time is expected to be even more reduced in a future 3D adaptive flow concept.

For a possible 3D adaptive flow concept, optimized definitions for detection functions may be implemented to allow next to areas of interest localization a better fluid pattern recognition in the additional dimension.

## ACKNOWLEDGEMENTS

The authors would like to express their gratitude to the technical support personnel of the Turbomachinery Laboratory and in particular to Cornel Reshef for his help and advice in the numerous issues of Electronic Engineering that arose during the course of the 2D Algorithm development. We would also like to extend our thanks to Thomas Behr and Luca Porreca for the installation and the operation of the axial research facility LISA.

## REFERENCES

- [1] Lienert A 2003 Automated Progressive Traversing of Fast Response Probes in Unsteady Turbomachinery Flow *Semester Thesis Turbomachinery Laboratory ETH Zurich*
- [2] Marti M 2003 Experimental Investigation of Unsteady Flow in an Axial Fan Using Fast Response Aerodynamic Probes *Semester Thesis Turbomachinery Laboratory ETH Zurich*
- [3] Oschwald M 2003 Experimental Investigation of Unsteady Flow Fields using a Progressive Traversing Algorithm *Semester Thesis Turbomachinery Laboratory ETH Zurich*
- [4] Lenherr C 2004 Experimental Investigation of Smart Probe Concept for Unsteady Flows in Axial Turbines (LISA) *Diploma Thesis Turbomachinery Laboratory ETH Zurich*
- [5] Behr T, Porreca L, Mokulys T, Kalfas A I, Abhari R S 2004 Multistage Aspects and Unsteady Effects of Stator and Rotor Clocking in an Axial Turbine with Low Aspect Ratio Blading *ASME Paper No. GT 2004-53612 Vienna*
- [6] Denton J D 1993 Loss Mechanisms in Turbomachines *ASME Journal of Turbomachinery Vol. 115 pp 621-656 October*
- [7] Sharma O P, Picket G F, Ni R H 1992 Assessment of Unsteady Flows in Turbines *ASME Journal of Turbomachinery Vol. 114 pp 79-90 and ASME Paper No. 90-GT-150*
- [8] Doorly D J 1988 Modeling the Unsteady Flow in a Turbine Passage *ASME Journal of Turbomachinery Vol. 110 pp 27-37 and ASME Paper No. 87-GT-197*
- [9] Thompson J F, Soni B K, Weatherill N P 1998 Handbook of Grid Generation *ISBN 0849326877 CRC Press*
- [10] Kalfas A I, Elder R L 1995 Determination of the Intermittency Distribution in the Boundary Layer of a Flat Plate with C4 Leading Edge *ERCFTAC Bulletin No 24 on Transition pp 65-67*
- [11] Binder A, Romey R 1983 Secondary Flow Effects and Mixing of the Wake behind a Turbine Stator *ASME Journal of Turbomachinery 105 pp 40-46*
- [12] Treiber M, Kupferschmied P, Gyarmathy G 1998 Analysis of error propagation arising from measurements with a miniature pneumatic 5-hole probe *Proc. 14th Symposium on Measuring Techniques for Transonic and Supersonic Flows in Cascades and Turbomachines, Limerick, Ireland*
- [13] Schlienger J, Pfau A, Kalfas A I, Abhari R S 2002 Single Pressure Transducer Probe for 3D Flow Measurements *The 16th Symposium on Measuring Techniques in Transonic and Supersonic Flow in Cascades and Turbomachines, Cambridge, UK*
- [14] Tanaka K, Kalfas A I, Hodson H P 2000 Development of Single Sensor Fast Response Pressure Probes *XVth Symposium on Measuring Techniques in Transonic and Supersonic Flows in Cascades and Turbomachines Florence Italy*
- [15] Gossweiler C R, Kupferschmied P, Gyarmathy G 1994 On Fast-Response Probes, Part 1: Technology, Calibration and Application to Turbomachinery *ASME Paper No. 94-GT-026 The Hague*
- [16] Humm H, Gossweiler C R, Gyarmathy G 1994 On Fast-Response Probes, Part 2: Aerodynamic Probe Design Studies *ASME Paper No. 94-GT-027 The Hague*
- [17] Kupferschmied P, Köppel P, Roduner C, Gyarmathy G 2000 On the Development and Application of the Fast-Response Aerodynamic Probe System in Turbomachines - Part 1: The Measurement System *ASME Journal of Turbomachinery Vol. 122 issue 3 pp 505-516*
- [18] Schlienger J, Pfau A, Kalfas A I, Abhari R S 2003 Measuring Unsteady 3D Flow with a single pressure transducer *Proceedings of the 5th European Turbomachinery Conference, Paper No TM02/63, pp.849-858*